Range Doppler Dynamic Range Considerations for Dechirp on Receive Radar

Josias J. de Witt #1, Willem A.J. Nel #2

#Council for Scientific and Industrial Research (CSIR), Pretoria, South Africa
[1]jdewitt@csir.co.za [2]wajnel@csir.co.za

***Abstract*— A dechirp on receive (DoR) concept demonstrator was recently implemented on the Fynmeet radar system of the CSIR, in an attempt to extend its high range resolution (HRR) measurement capabilities. Based on the low dynamic range observed in subsequent measurements, this paper presents detailed analysis of the effect of amplitude, phase and nonlinear distortion on dechirp on receive radars.**

I. Introduction

The need for high range resolution (HRR) measurement capabilities are becoming increasingly important in the analysis of target radar cross section (RCS) contributors, especially in the field of non-cooperative target recognition. The Fynmeet radar system of the CSIR, currently its main RCS measurement facility, has been using an HRR measurement technique based on stepped frequency waveforms (see eg. [1]), which limits the achievable Doppler bandwidth.

Dechirp on receive is a method to achieve HRR measurements of a target with a limited range extent, within a single pulse, while reducing the requirements on the amount of intermediate frequency (IF) bandwidth required [2]. It involves transmitting a wideband, linear frequency modulated (LFM) pulse and mixing the echo returns with a accurately timed, pulsed, LFM local oscillator (LO) signal with the same chirprate. This is referred to as 'deramping' the received signal.

In January 2007 a dechirp on receive concept demonstrator was implemented in the Fynmeet system. This implementation illustrated the successful integration of the technique, however the spurious free dynamic range (SFDR) of the measurements was poor (only about 20 dBs). This prompted an in-depth study into hardware front-end factors that affect the SFDR of dechirp on receive measurements.

Some of these contributing factors that have been analysed in literature include: range sidelobes (due to linear distortion of the amplitude and phase of the LFM signal [3], [4], [5]) and asymmetrical windowing effects [6]. In this paper we aim to extend the analysis of [3], [4], [5] by including the analysis of amplitude and phase distortion introduced by both the signal path shared by the transmit and LO LFM signals, as well as by the signal path which only affect the transmitted pulse (Section IV-A). Such a scenario is encountered in the implementation in the Fynmeet system. Furthermore this paper presents detailed analysis of the effect of nonlinear distortion, in the form of in-band harmonics, and intermodulation distortion (IMD), on dechirp on receive measurements in the range-Doppler domain (Section IV-B).

II. Mathematical modeling of Dechirp Processing

We start by writing the expression for the LFM LO signal as

$$s_{LO}(t) = A_1 \cos[\omega_1 t + a/2t^2] \tag{1}$$

where A_1 denotes the amplitude, ω_1 the centre frequency in rad/s and a the chriprate in rad/s^2. We model the echo return from a point scatterer at a range of $c\Delta t/2$ meters, relative to the centre of the range extent (range scene centre), as a scaled and delayed version of the transmitted chirp pulse. Let this echo of length T_0 seconds be denoted by

$$\begin{aligned} s_R(t) &= A_2 \cos[\omega_2(t-\Delta t) + a/2(t-\Delta t)^2]\,; \\ &\quad -T_0/2 \le t \le T_0/2\,. \end{aligned} \tag{2}$$

The output of the deramping process yields

$$\begin{aligned} y(t) &= s_R(t)s_{LO}(t)\,;\ -T_0/2 \le t \le T_0/2 \\ &= \underbrace{\frac{A_1A_2}{2}\cos\left[(\omega_1-\omega_2+a\Delta t)t - \frac{a}{2}\Delta t^2 + \omega_2\Delta t\right]}_{\text{Desired component}} \\ &\quad + \underbrace{\frac{A_1A_2}{2}\cos\left[(\omega_1+\omega_2-a\Delta t)t + at^2 + \frac{a}{2}\Delta t^2 - \omega_2\Delta t\right]}_{\text{Unwanted component}} \end{aligned} \tag{3}$$

The unwanted double frequency component in (3) is normally removed through analogue filtering, resulting in a single frequency signal

$$y_{IF}(t) = A' \cos(\omega' t + \phi')\,, \tag{4}$$

where $A' = A_1A_2/2$, $\omega' = \omega_1 - \omega_2 + a\Delta t$ and $\phi' = -a\Delta t^2/2 + \omega_2\Delta t$. Pulse compression is now achieved through spectral analysis. The Fourier transform of (4) is given by

$$Y_{IF}(\omega) = C\text{sinc}[(\omega'+\omega)T_0/2\pi] + C^*\text{sinc}[(\omega'-\omega)T_0/2\pi] \tag{5}$$

where $C = A'T_0\exp(j\phi')/2$. This represents two sinc functions centred around $\pm\omega$ rad/s, each with a mainlobe width of $2/T_0$ Hz.

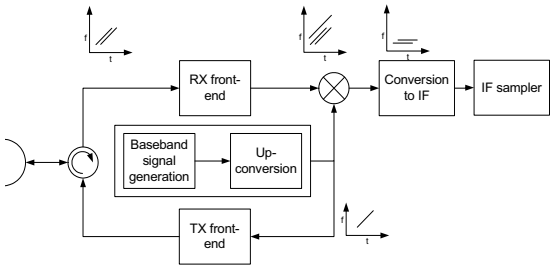

Fig. 1. Simplified block diagram of the dechirp on receive implementation in Fynmeet.

III. Implementation in the Fynmeet Radar system

A. System overview

Fig. 1 shows a simplified block diagram of the Fynmeet dechirp on receive implementation. The baseband LFM pulses are generated through direct digital-to-analogue conversion, at a centre frequency of 250 MHz. The transmit signal has a bandwidth of 400 MHz. Both the transmit and LO LFM signals are translated to X-band. The LO LFM chirp signal drives the LO port of a RF mixer which mixes it with the received signal. The desired frequency components are isolated through bandpass filtering and mixed down to an IF frequency of 100 MHz,with bandwidth of 10 MHz. This IF signal is then sampled by the intermediate frequency sampling (IFS) subsystem at a rate of 125 MSPS and quadrature down-converted to 0 Hz in the digital domain. Windowing and FFT processing then yields the desired range profile.

B. Measurement results

A measurement trial was performed to test the dechirp on receive implementation in Fynmeet. Two point-like scatterers, a corner reflector and conducting sphere, were suspended diagonally to the ground, with a rope, from the top of a nearby tower. The range separation of the two targets were about 1.5 m. To achieve separation from stationary clutter return through Doppler processing, the sphere was swung to and fro, relative to the radar. This motion also coupled through to the corner reflector. Fig. 2 shows the range-Doppler map of

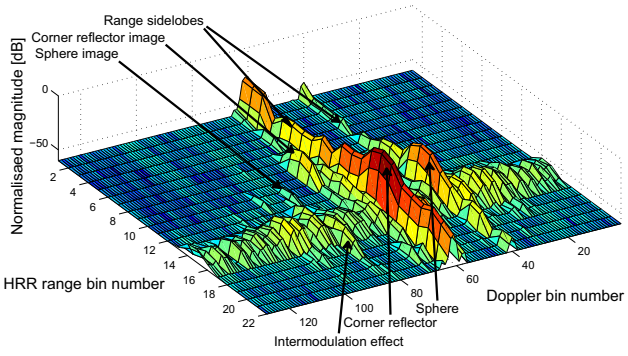

Fig. 2. Range-Doppler map of two point scatterers (range bins 12 and 14) measured with the Fynmeet dechirp on receive implementation.

the two scatterers. It is seen that although the two targets can indeed be resolved, the spurious free dynamic range (SFDR) of the measurements are severely reduced by a number unwanted artifacts.

IV. Dynamic Range Considerations

A. Range sidelobes due to amplitude and phase distortion

1) Nonlinear phase response: The authors of [3], [4] analyse the case where phases of the transmit and LO LFM pulses are distorted by the same signal path. To fully model the scenario in Fynmeet, this analysis is extended to include a secondary distortion, affecting the transmitted pulse.

The distorted return from a point scatterer can be written as

$$S'_R(t) = A_2 \cos[\omega_2(t-\Delta t) + a/2(t-\Delta t)^2 + \theta(t-\Delta t) + \varphi(t-\Delta t)] \quad (6)$$

where $\theta(t)$ and $\varphi(t)$ denote the phase error terms. $\theta(t)$ denotes the common phase error, while $\varphi(t)$ affects only the transmitted signal. Accordingly, the distorted LO LFM signal is given by

$$S'_{LO}(t) = A_1 \cos[\omega_1 t + a/2t^2 + \theta(t)] \quad (7)$$

After deramping and bandpass filtering the target return, the IF signal is given by

$$y'_{IF}(t) = A' \cos[\omega' t + \phi' + \theta(t) - \theta(t-\Delta t) - \varphi(t-\Delta t)] \quad (8)$$

We may write $\theta(t)$ and $\varphi(t)$ in terms of their most significant Fourier series component to simplify the analysis, as was done in [3] and [4]. Thus we let $\theta(t) = \theta_p \cos(\omega_\theta t)$ and $\varphi(t-\Delta t) = \varphi_p \cos(\omega_\varphi t)$. Since we can assume that normally $2\pi/\omega_\theta >> \Delta t$ [3], we can make the approximation that [3]

$$\theta(t) - \theta(t-\Delta t) = \Delta t \frac{d\theta(t)}{dt} = -\Delta t \theta_p \omega_\theta \sin(\omega_\theta t) = \beta \sin(\omega_\theta t) \quad (9)$$

where $\beta = -\Delta t \theta_p \omega_\theta$. Using the approximation of (9), a slightly different form of (8) may be written as

$$y'_{IF}(t) = A' \mathrm{Re}\{\exp j[\omega' t + \phi'] \times \exp j[\beta \sin(\omega_\theta t)] \exp j[\varphi_p \cos(\omega_\varphi t)]\} \quad (10)$$

In the above equation, the expression $\exp j[\beta \sin(\omega_\theta t)]$ can be expanded into a series using Bessel functions, as [3]

$$\exp j[\beta \sin(\omega_\theta t)] = \sum_{n=-\infty}^{\infty} J_n(\beta) \exp(jn\omega_\theta t) \quad (11)$$

where $J_n(.)$ denotes the Bessel function of the first kind, order n. The factor $\exp j[\varphi_p \cos(\omega_\varphi t)]$ can be expanded into a series, using the Jacobi-Anger Expansion (see e.g. [7, p. 681]), as

$$\exp j[\varphi_p \cos(\omega_\varphi t)] = \sum_{m=-\infty}^{\infty} j^m J_m(\varphi_p) \exp(jm\omega_\varphi t) \quad (12)$$

Using the series representation of (11) and (12), a typical magnitude spectrum of a point scatterer return, when nonlinear phase distortion exists, is depicted in Fig. 3. The expressions for the relative strengths of the sidelobes, follow directly when

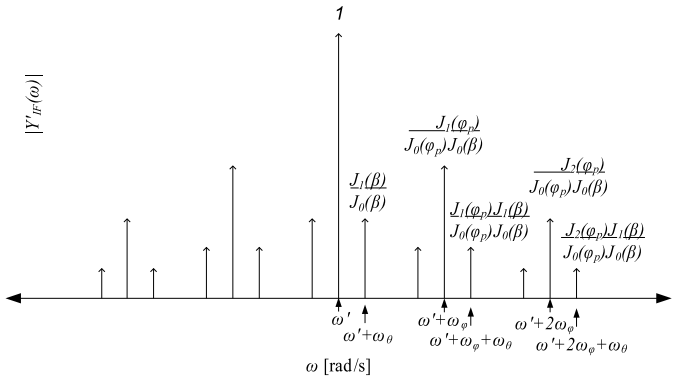

Fig. 3. Normalised one-sided magnitude spectrum of the dechirped IF signal in the presence of nonlinear phase distortion. (*Sinc* envelopes not shown; line lengths illustrate a typical scenario.)

expanding the first two terms of (11) and the first three terms of (12).

The maximum value of β is related to the available IF bandwidth (B_{IF} in Hz) as $\max[\beta] = -2\pi B_{IF}\theta_p/\Delta f_\theta$, if we let $\Delta f_\theta\,(= a/\omega_\theta)$ denote the frequency span (in Hz) of one period of the phase error function. Considering the Fynmeet implementation, it is seen that for slowly varying phase error functions, φ_p will typically be larger than β when φ_p and θ_p are of comparable sizes. This is due to the fact that β experiences a cancelling effect when the target return and the LO LFM signals align in time. For a range sidelobe level (RSL) of -40 dB, the maximum allowable value for φ_p is about 1 degree. This is stricter than the specifications on θ_p of about 3.6 degrees for the Fynmeet implementation (assuming $\Delta f_\theta \approx 200$ MHz).

2) Non-flat Amplitude Response: We model the effect of a non-flat amplitude response by making the amplitude scaling terms of the filtered IF signal in (4), time variant. We define

$$A_1'(t) = A_1[1 + \epsilon(t)] \tag{13}$$

$$A_2'(t - \Delta t) = A_2[1 + \epsilon(t - \Delta t) + \kappa(t - \Delta t)] \tag{14}$$

where $\epsilon(t)$ denotes the amplitude error function introduced by the signal path shared by both signals, while $\kappa(t)$ denotes the error affecting only the transmitted signal. As suggested in [3], we may once again write $\epsilon(t)$ and $\kappa(t)$ in terms of their most significant Fourier components such that $\epsilon(t) = \epsilon_p \cos(\omega_\epsilon t)$ and $\kappa(t - \Delta t) = \kappa_p \cos(\omega_\kappa t)$. By expanding the product $A_1(t)A_2(t - \Delta t)$ we have that

$$\frac{A_1(t)A_2(t - \Delta t)}{A_1 A_2} \approx 1 + 2\epsilon_p \cos(\omega_\epsilon t) + \kappa_p \cos(\omega_\kappa t) \tag{15}$$

In the above expression the contributions of ϵ_p^2 and $\epsilon_p\kappa_p$ terms were ignored and it was assumed that $\omega_\epsilon \Delta t << 1$. The AM components at $\omega = \omega' \pm \omega_\epsilon$ and $\omega = \omega' \pm \omega_\kappa$ rad/s will have relative strengths of ϵ_p and $\kappa/2$, respectively, relative to the desired component. It is seen that, unlike phase error, the amplitude distortion's effect is worsened in the event where the same distortion is applied to both the transmit chirp and LO signals. As an example, for a RSL of less than -40 dB, the amplitude response of the analogue front-end should have a ripple (ϵ_p) of less than 1%.

B. Nonlinearity

Passing the transmit or LO LFM signal through a nonlinear transfer function will result in false replicas of existing targets appearing in the range-Doppler map. We will use a Taylor series expansion to model the effect of frequency-independent, memoryless nonlinearities. Using this model, the output of a nonlinear device can written in terms of its input $x(t)$ as [8]

$$y(t) = \sum_{k=0}^{N} a_k x^k(t) \tag{16}$$

where k indicates the harmonic number (fundamental is $k = 1$) and a_k the weighting, which is device dependent.

1) In-band Harmonic Distortion: In-band harmonic distortion refers to the case where harmonics of the fundamental signal falls within its own frequency band. This may occur when the bandwidth of the signal is large compared to its centre frequency, as is the case at the first mixing stage of the baseband signal. In such a case the harmonic content cannot be removed though filtering.

We model the nonlinear behaviour of the first mixing stage as the multiplication of two signals that were each passed through a nonlinear device [9].

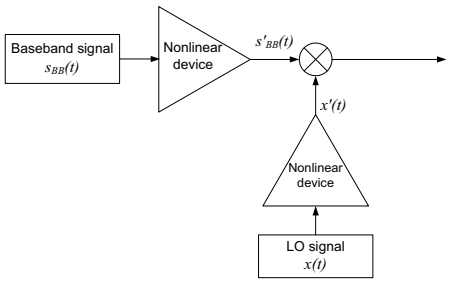

Fig. 4. Model for the harmonic distortion of the first mixing stage of the Fynmeet implementation.

Using this model, as illustrated in Fig. 4, the baseband signal $s'_{BB}(t)$ can be written as

$$s'_{BB}(t) = \sum_{n=0}^{N} K_n \cos[n\phi_{BB}(t)] \tag{17}$$

where K_n is a function of multiple Taylor coefficients and $\phi_{BB} = \omega_{BB}t + a/2t^2$ represents the baseband LFM signal's phase function. Similarly, the distorted LO signal can be written as

$$x'(t) = \sum_{m=0}^{M} G_m \cos(m\omega_x t) \tag{18}$$

where ω_x indicates the frequency of the LO, which is usually much larger than the bandwidth of the LFM signal. Since the product of these two terms is followed by an analogue band-pass filter, isolating components in the region of $\omega_x + \omega_{BB}$,

we may write its output as

$$d_{\text{filter}}(t) = \text{BPF}\{s'_{BB}(t)x'(t)\} = \sum_{n=1}^{R} K_n \cos[n\phi_{BB}(t) + \omega_x t] \quad (19)$$

where R ($< N$) now indicates the number of in-band harmonics that could not be removed though filtering. This signal will typically pass through more mixing and filtering stages before being transmitted. However, the nonlinear distortion of these stages will usually result in harmonics that are far removed from the fundamental and are thus easily removed through filtering. Using the definitions of (1) and (2), we can now write the return from a point target and the dechirp LO signal, respectively, as

$$s'_R(t) = \sum_{n=1}^{R} K_n \cos[n\phi_{BB}(t-\Delta t) + (\omega_2 - \omega_{BB})(t-\Delta t)]$$
$$s'_{LO}(t) = \sum_{n=1}^{R} K_n \cos[n\phi_{BB}(t) + (\omega_1 - \omega_{BB})t]\,. \quad (20)$$

The IF signal, after deramping and bandpass filtering, is then given by

$$y'_{IF} = K_0^2 \cos(\omega_1 t - \omega_2 t + \Delta t \omega_2) + 1/2 \sum_{n=1}^{R} K_n^2 \cos[\theta(t,n)] \quad (21)$$

where

$$\theta(t,n) = [na\Delta t + \omega_1 - \omega_2]\, t + \left[n(\omega_{BB}\Delta t - a\Delta t^2/2) + (\omega_2 - \omega_{BB})\Delta t\right] \quad (22)$$

In the above expression, only the component corresponding to $n = 1$ is desired. It is seen that in-band harmonic distortion causes false target returns to appear at integer multiples of the true targets range, relative to the centre of the measurement range extent. However, since the dominating phase term $(\omega_2 - \omega_{BB})\Delta t$ is not affected by n, these false returns would essentially reside in the same Doppler bin as the true target return, when Doppler processing is performed on a moving target. Their energy can be reduced by applying a bandpass filter to the fundamental component's frequency band.

2) Intermodulation Effects: Intermodulation distortion (IMD) will occur when two target returns overlap in time (ie. multiple frequencies exist in the receive path at the same time instance) and are passed though a nonlinear device. For illustrative purposes, we investigate the effect of third order intermodulation products (IMP).

The in-band third order IMP of two signals $A_1 \cos(\phi_1(t))$ and $A_2 \cos(\phi_2(t))$ will reside at frequencies resulting from the expressions $2\phi_1(t) - \phi_2(t)$ and $2\phi_2(t) - \phi_1(t)$. Let us define $\phi_1(t)$ and $\phi_2(t)$ to be the phase functions (similar to the expression of (2)) of the returns from two targets at ranges of $c\Delta t_1/2$ and $c\Delta t_2/2$ meters, respectively. It can be shown that irrespective of whether the composite return signal is passed through a non-linearity before decamping with the LFM LO or after the decamp process, the filtered IF signal will additionally contain the following IMPs:

$$\text{IMP}_1 = \frac{3a_3 A_1^2 A_2}{8} \cos\Big\{ [\omega_1 - \omega_2 + a(2\Delta t_1 - \Delta t_2)]\, t + \omega_2(2\Delta t_1 - \Delta t_2) - a/2(2\Delta t_1^2 - \Delta t_2^2) \Big\} \quad (23)$$

$$\text{IMP}_2 = \frac{3a_3 A_2^2 A_1}{8} \cos\Big\{ [\omega_1 - \omega_2 + a(2\Delta t_2 - \Delta t_1)]\, t + \omega_2(2\Delta t_2 - \Delta t_1) - a/2(2\Delta t_2^2 - \Delta t_1^2) \Big\} \quad (24)$$

where a_3 denotes the third order Taylor coefficient of the nonlinear transform function. It is seen that intermodulation will cause target returns to mirror around each other, not only in range (false targets at $c(2\Delta t_1 - \Delta t_2)/2$ and $c(2\Delta t_2 - \Delta t_1)/2$ meters) but also, in the case of moving targets, in the Doppler domain, due to the phase terms $\omega_2(2\Delta t_1 - \Delta t_2)$ and $\omega_2(2\Delta t_2 - \Delta t_1)$. These components will contain less energy than the desired components, since they exist only during the time that target returns overlap.

V. Conclusions

This paper presented detailed analysis of the dynamic range implications of front-end amplitude and phase as well as nonlinear distortion, in a dechirp on receive systems. Explicit expression were provided to aid in the design of front-end specifications for such radars. All of the effects presented in this paper were considered major contributing factors to the low SFDR of the dechirp measurements with the Fynmeet radar system.

Acknowledgment

This research was funded by Armscor under contract no. KT521888. The authors would like to thank the digital design team at CSIR DPSS for the use of their DRFM hardware.

References

[1] G. Gill, "Simultaneous pulse compression and doppler processing with step frequency waveform," *IEEE Electronics Letters*, vol. 32, pp. 2178–2179, Nov 1996.

[2] J. Blanton, "Cued medium-PRF air-to-air radar using stretch range compression," *Proceedings of the 1996 IEEE National Radar Conference*, pp. 208–213, 13-16 May 1996.

[3] B. W. Griffiths, "Digital generation of high time-bandwidth product linear FM waveforms for radar altimeters," *IEE Proc. on Radar and Signal Processing*, vol. 139, pp. 160–169, 1992.

[4] R. Xu, Z. Cao, and X. Liu, "Compensation for distorted LFM signal," *Proc. of the IEEE 1993 National Aerospace and Electr. Conf. (NAECON 1993)*, vol. 1, pp. 61–66, May 1993.

[5] M. Belcher, R. Howard, and M. Mitchell, "Modulation error in active-aperture phased-array radar systems," *International Radar Conference*, pp. 9–12, 12-13 Oct 1992.

[6] Z. Yang, J. Ni, and G. Liu, "Delay compensation of stretching signal in OTHR," *6th International Conference on Signal Processing*, vol. 2, pp. 1461 – 1464, 26-30 Aug 2002.

[7] G. Arfken and H. Weber, *Mathematical Methods for Physicists*, 5th ed. Harcourt/Academic Press, 2000.

[8] X. Zeng, Q. Hu, J. He, Q. Tu, and X. Yu, "High power RF amplifiers new nonlinear models," *Microwave Conference Proceedings, 2005. APMC 2005. Asia-Pacific Conference Proceedings*, vol. 2, no. 4-7, Dec 2005.

[9] J. Witkowsky, "A hardware emulator testbed for a software-defined radio," Master's thesis, University of Stellenboschy, South Africa, 2003.